Single-Molecule Tracking of Fibrinogen Dynamics on Nanostructured Poly(ethylene) Films

*Mark Kastantin, Thomas F. Keller, Klaus D. Jandt, and Daniel K. Schwartz**

Using fibrinogen (Fg) protein as a probe molecule, mapping using accumulated probe trajectories (MAPT) is performed on nanostructured melt-drawn high-density poly(ethylene) (HDPE) films composed of well-oriented crystalline patches separated by amorphous regions. The spatially grouped molecular trajectories allow for identification of regions with distinct surface properties (i.e., crystalline vs. amorphous) while simultaneously determining the characteristic dynamic protein behavior within those regions. In the presence of solution with a sufficiently high Fg concentration, discrete patches of a dense, ordered protein layer form (presumably on crystalline HDPE regions), leading to a dramatic rise in the surface residence time (by more than two orders of magnitude) of molecules incorporated into the film. Within this ordered Fg layer, individual molecules exhibit slow anisotropic lateral diffusion; the mobility is restricted by the nanostructure boundaries of the underlying HDPE. On HDPE films at low Fg surface coverage, or on films that have been rendered hydrophilic with Ar plasma, short surface residence times and fast, isotropic diffusion are observed. These results demonstrate the ability of spatially resolved single-molecule tracking to provide mechanistic information about biomolecule-surface interactions in a highly heterogeneous environment.

1. Introduction

It is increasingly clear that subtle properties of a surface in contact with a biological fluid (e.g., blood, synovial fluid, etc.) can alter the behavior of proteins adsorbing to that surface and the properties of the resulting protein layer. The amount, conformation, and orientation of adsorbed proteins can be dramatically affected by surface properties such as chemistry,[1–4] crystallinity,[5,6] topography,[7–10] and nanoscale surface asymmetry.[11] Furthermore, the properties of the adsorbed protein layer can dramatically affect the cellular response to the material. For example, in the work of Coelho et al., type IV collagen that adsorbed onto $-NH_2$ functionalized surfaces formed a network of elongated fibrils that supported the formation of stable focal adhesions and resulted in cell adhesion and spreading on these surfaces.[1] In contrast, no such fibrils were observed on –COOH functionalized surfaces, leading to poor cell adhesion and spreading.

While there is ample evidence indicating that a relationship exists between surface properties and material function, the mechanisms of the underlying interactions are poorly understood on the molecular level, frustrating attempts to harness these properties for bottom-up design of implanted biomaterials. Protein-surface interactions may be relatively subtle and may change dynamically, making these systems difficult to study. For example, atomic force microscopy (AFM) can provide single-molecule resolution and sensitivity to the nanometer-scale topography of both the protein layer and the underlying surface. However, topographic maps of a surface provided by AFM can be difficult to interpret in complex protein layers and the time resolution is often slow compared to the dynamics of interest.

Here, we use a technique recently developed in our laboratory, mapping using accumulated probe trajectories (MAPT),[12,13] to obtain in situ information on the dynamics of fibrinogen (Fg) on nanostructured melt-drawn high density poly(ethylene) (HDPE) films. MAPT generates images of surface interactions with probe molecules by grouping different aspects of many single-molecule trajectories by their spatial location with super-resolution precision. Unlike other super-resolution techniques that report only photon or point counts,[14–17] this technique generates surface maps of physical quantities (desorption probability, local surface diffusion coefficient, surface occupancy, etc.) that directly report on probe-surface interactions. Importantly for this work, the single-molecule basis for MAPT provides excellent sensitivity to heterogeneous Fg behavior as Fg interactions with nanostructured HDPE films can vary greatly due to both underlying surface heterogeneity and the multiple types of Fg interactions with even a uniform surface.

Although MAPT requires dilute concentrations of fluorescently labeled molecules to attain single-molecule spatial

Dr. M. Kastantin, Prof. D. K. Schwartz
Department of Chemical and Biological Engineering
University of Colorado Boulder
Boulder, CO 80309, USA
E-mail: daniel.schwartz@colorado.edu
Dr. T. F. Keller, Prof. K. D. Jandt
Institute of Materials Science & Technology (IMT)
Friedrich-Schiller-University Jena
Löbdergraben 32, 07743 Jena, Germany
Prof. K. D. Jandt
Jena Center for Soft Matter (JCSM)
Friedrich-Schiller-University Jena,
Löbdergraben 32, 07743 Jena, Germany

DOI: 10.1002/adfm.201102836

resolution, dense protein layers can be studied by introducing a trace amount of fluorescently labeled protein of interest into an otherwise unlabeled protein layer.[18] The labeled probe molecules can subsequently report on their local environment, yielding single-molecule information on properties of the layer. In multicomponent systems that are representative of physiological environments, the labeled species can be varied in order to study the contribution of each component separately. Thus, MAPT has promise as a powerful in situ tool with which to probe mechanistic questions that link nanoscale material properties with material function.

Poly(ethylene) (PE) of different grades is widely used in the biomedical field, e.g., for sutures[19] or endoprosthetic devices.[20–22] Similar to the ultrahigh molecular weight variant (UHMWPE), HDPE is a semicrystalline thermoplastic consisting of crystalline, chain-folded lamellae that impart nanoscale topography to the film. HDPE was chosen over UHMWPE in this work for its greater macroscale uniformity with respect to the formation and orientation of crystalline lamellae. Recently, melt-drawn films of either HDPE or UHMWPE were demonstrated to form nanostructured surfaces.[23] Rectangular crystalline domains (~30 nm × 100 nm) protruded a few nanometers out of the interconnecting amorphous region.[11] These domains arranged themselves in a highly oriented way with their crystalline lamellae thickness aligned parallel to the drawing direction. Films with this crystalline nanostructure demonstrated the ability to template the orientation of adsorbed layers of rodlike macromolecules such as Fg or alpha helical poly(lysine)/poly(styrene sulfonate) complexes.[11,24]

The ability of nanostructured polymer films to template ordered Fg layers has practical interest due to the ability of adsorbed proteins to lubricate the surfaces of implanted biomaterials and reduce wear on artificial joints.[2] Although much research has focused on the lubricating properties of serum albumin, relatively high Fg concentrations are present in the synovial fluid of osteoarthritics.[25] Successful lubrication, however, is dependent on the specific interactions between the biomaterial surface and a protein. For example, although native serum albumin is typically viewed as a natural lubricant, it can actually decrease the wear resistance of UHMWPE whose chains have been oriented by uniaxial compression or stretching[26] relative to these biomaterials in pure water[27] or the dry state.[28] This phenomenon has been attributed to the accumulation of denatured protein at the interface, which leads to increased friction,[29] and highlights the type of molecular level insights that are required to understand the behavior of these materials. Thus in the present work, Fg adsorption onto nanostructured HDPE films serves both as a model system for the MAPT technique and as a system of practical importance for the molecular understanding of lubrication via adsorbed protein layers in polymeric implants.

In a previous study of Fg orientation on UHMWPE films using AFM, proteins were observed to self-assemble into a well-ordered arrangement.[24] This oriented arrangement was observed only at high surface densities of Fg and was not observed on films that had been treated with Ar plasma after melt-drawing, even at high Fg surface density. In the context of implanted biomaterials, these static observations of Fg layer structure under different conditions raise questions about the dynamic properties of proteins in the layer. That is, does molecular orientation impart stability to the layer and are molecules fixed or mobile within the plane of the layer? In the present work, MAPT addresses these questions by directly measuring the spatial dependence of surface residence times and diffusion coefficients of Fg in adsorbed protein layers.

2. Results and Discussion

2.1. MAPT Identifies Elongated Structures on HDPE Film

Melt-drawn HDPE films were exposed to aqueous solution that contained 5×10^{-4} mg L^{-1} of fluorescently labeled human Fg and, optionally, 10 mg L^{-1} of unlabeled human Fg. Labeled Fg was tracked and the molecular trajectories were used to map the film surface. A representative surface occupancy map of the HDPE film exposed to 10 mg L^{-1} Fg is shown in **Figure 1** where surface occupancy is defined in the Experimental Section.

While Fg molecules were observed to explore large areas of the film, distinct areas of extremely high occupancy were observed that were elongated in the drawing direction (indicated by arrows in Figure 1a). These structures were roughly ~1 μm in length by ~0.1 μm wide and were sometimes segmented into smaller regions along their length (Figure 1b–e). Occasionally, bifurcations in the structures were observed

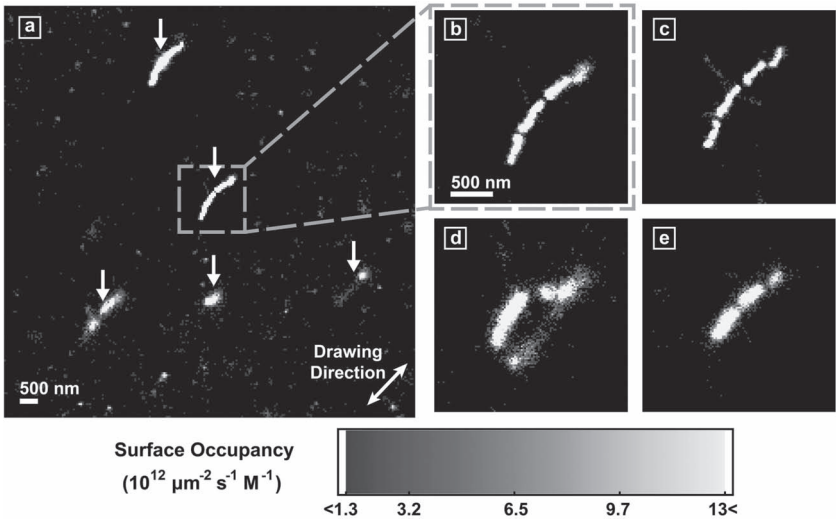

Figure 1. Occupancy map of HDPE film at 10 mg L^{-1} Fg concentration. a) Several features are observed with both high surface occupancy and elongation in the film drawing direction. Arrows indicate these structures, which have varying aspect ratios. b) One of the elongated features in (a) is magnified 2.5×. c–e) Representative structures from areas of the film that are not shown in (a) are shown on the same scale as (b).

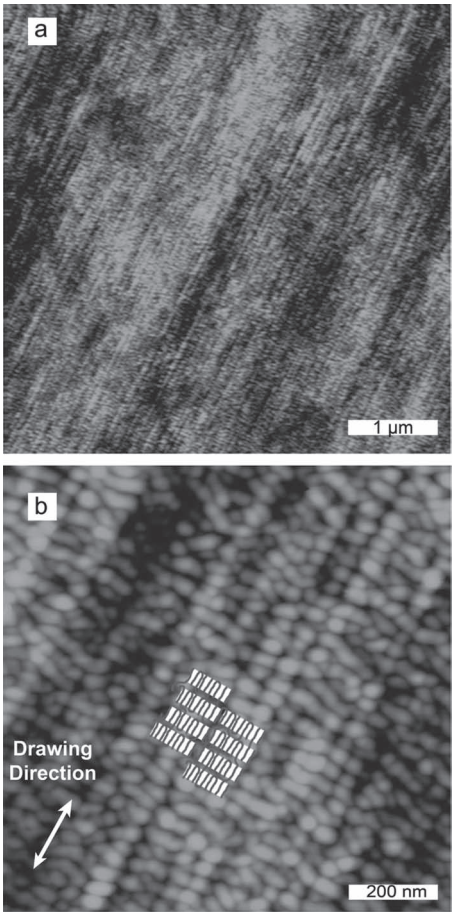

Figure 2. Topographic AFM image of hydrophobic HDPE film. a) A representative image shows that oriented crystalline lamellae cover a large area fraction of the film surface. b) Film structure is shown with higher magnification in order to show details of the nanoscale topography. The cartoon overlay indicates the orientation of crystalline lamellae that protrude out of the amorphous film. The color range from black to light gray represents a height difference of 20 nm.

(Figure 1d) where Fg did not explore an area between two elongated regions. Overall, the geometry of these high occupancy areas did not directly correspond to that of crystalline lamellae as seen using AFM in **Figure 2**. For example, segmentation of elongated regions, seen in Figure 1b–d, were not apparent from topographic images of the film in Figure 2. Thus, one advantage of the MAPT technique is that it can identify regions of connectivity from the perspective of an adsorbate molecule that are not necessarily apparent from purely topographical images. It would be interesting for future work to address what properties of the film lead to these elongated, but segmented molecular trajectories.

Figure 3 shows an analogous MAPT image obtained on an HDPE film that had been treated with Ar plasma to render it hydrophilic (referred to in the figures as Pl-HDPE film). The total Fg concentration was again 10 mg L^{-1}. While areas of high occupancy were still observed (Figure 3a), these areas were compact in shape, unlike the elongated areas on the untreated, hydrophobic HDPE film in Figure 1. This is despite that fact that previous AFM characterization of these films has shown that plasma treatment at the applied conditions does not alter the semicrystalline structure of the film.[24] Interestingly, when a hydrophobic HDPE film was exposed to only labeled Fg at 5×10^{-4} mg L^{-1}, the resulting occupancy maps (Figure 3b) resembled those of the hydrophilic HDPE film rather than the hydrophobic HDPE film in Figure 1. Thus, both hydrophobic HDPE and high Fg concentration were required for the appearance of elongated structures on semicrystalline melt-drawn films. These results are consistent with a previous AFM characterization of Fg adsorption onto UHMWPE films in which oriented protein layers formed only on hydrophobic films at high total Fg concentration (10 mg L^{-1}).[24] Thus, it seems likely that oriented Fg layer formation is responsible for the elongated occupancy structures.

One advantage of the MAPT approach is that molecular trajectories can be grouped according to spatial position and analyzed separately. In this work, this permits separate analysis of regions of high and low occupancy. Such a comparison can be useful when trying to isolate potentially rare and interesting events, such as protein behavior in an oriented layer, from more common protein-surface interactions.

2.2. Mean Residence Times

The mean surface residence times for areas of high and low occupancy on each surface are given in **Table 1**. The Fg mean residence time was shortest on treated hydrophilic HDPE surfaces, with values <1 s in both low and high occupancy areas even at high Fg concentrations, suggesting that plasma treatment slightly decreased the affinity of Fg for the HDPE surface. On hydrophobic HDPE surfaces, mean residence times were also relatively short within low occupancy areas at all Fg concentrations, although this value did increase slightly at high Fg concentration, suggesting that the presence of other Fg molecules may help to stabilize newly adsorbing Fg. Relative to hydrophilic HDPE, we also saw a modest increase in residence time in areas of high occupancy on hydrophobic HDPE at low Fg concentration, but a larger experimental uncertainty in this value obscures this result. Overall, these effects are relatively modest as indicated by the fact that mean residence times are all of order ~1 s.

Dramatically, the mean residence time increased by more than two orders of magnitude in areas of high occupancy on hydrophobic HDPE at high Fg concentration. The listed value of >160 s indicates that the majority of these objects were present for the duration of a single movie. In fact, most of these objects appeared in approximately the same spot in multiple consecutive movies but due to a lack of continuous tracking, we could not be certain that each represented the same Fg molecule. Nevertheless, it seems likely that the mean residence time in these areas is much greater than our conservative estimate of 160 s. This value is in stark contrast to mean residence times observed in all other instances in this work (i.e., areas of low occupancy or under different experimental conditions) and is also much longer than mean residence times of ~1 s that were observed for Fg monomers on bare fused silica, poly(ethylene glycol), or trimethylsilane surfaces.[30] The fact that areas of

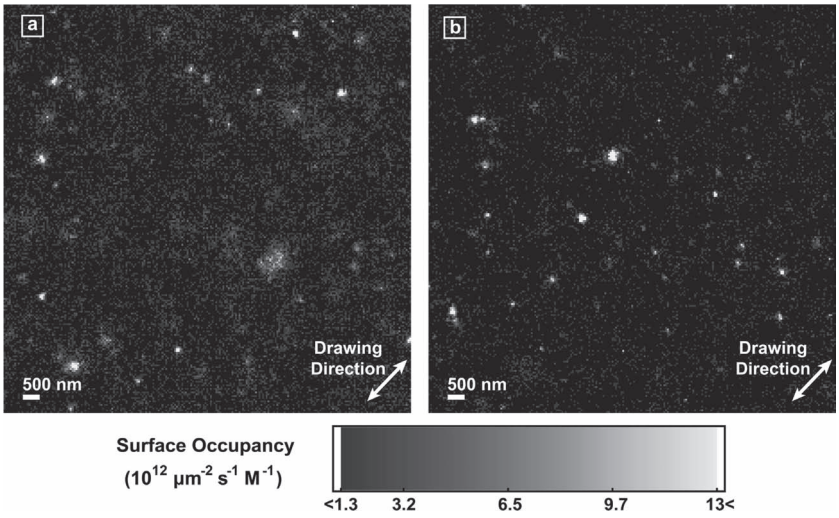

Figure 3. Occupancy map of HDPE films that do not exhibit elongated structures. a) Map of plasma-treated HDPE film exposed to 10 mg L^{-1} Fg concentration. b) Map of HDPE films exposed to labeled Fg at 5×10^{-4} mg L^{-1}. In both images, high occupancy areas are observed that are compact and roughly circular in shape.

elongated occupancy and extremely long residence times occur only under conditions known to form ordered Fg layers is strong evidence for the dominant effect of protein-protein interactions in determining the dynamic behavior of these layers.

Due to its role in clotting, there are numerous locations on Fg that lead to strong protein-protein interactions. For example, covalent γ_{xl}-γ_{xl} linkages can form between adjacent D domains on Fg while fibrinopeptide A can form a non-covalent bridge between the central E domain and a docking site on the D domain.[31] However, this conversion of Fg to a polymerizable fibrin monomer requires the enzymatic activation of various sites by thrombin. In the work of Chen et al., an Au(1,1,1) surface was able to induce Fg self-assembly in the absence of thrombin.[32] This was believed to be a result of the ability of Au to reductively break disulfide bonds, subsequently activating Fg. In the present work, we have neither thrombin nor Au to activate Fg and we have no reason to believe that HDPE has any significant effect on covalent Fg structure. Thus, we believe that the nature of protein-protein interactions in this work is predominantly non-covalent and that there is a link between spatial alignment and the strength of these non-covalent interactions. The fact that long Fg residence times are only observed under conditions that were shown via AFM to induce well-ordered Fg layers on nanostructured UHMWPE films[24] is strong indirect evidence that Fg alignment, and potentially stronger protein-protein interactions, is related to longer Fg residence times. Nevertheless, the molecular-level mechanisms that lead to both Fg alignment and subsequently long residence times require further study.

Despite the observation of high occupancy areas with elongated occupancy maps and long residence times, the vast majority of labeled Fg molecules was observed outside of these areas and had relatively short residence times. Our hypothesis for this observation is that the trajectories within elongated regions represented Fg molecules that were incorporated into the ordered layer while the short-lived molecules represented Fg that adsorbed onto the surface but was blocked from adopting an oriented, stable configuration by preexisting Fg on the surface. Given the fraction of labeled Fg in these experiments (5×10^{-5}), the dimensions of the PE lamellae, (~0.1 μm × 0.03 μm), and an approximate area fraction of crystalline lamellae on the film (~0.7), the observed surface density of ~2.7×10^{-2} labeled film-incorporated Fg molecules per μm^2 is consistent with a layer where 2–3 Fg molecules occupy a single lamella, a value that is roughly consistent with a Fg width of ~10 nm.[33] This idea of a close-packed, ordered layer of Fg supports the claim that protein-protein interactions are primarily responsible for stabilizing the protein layer. In these experiments, the maximum concentration of fluorescent Fg was limited by the steady-state surface density of Fg; larger fractions of probe molecules led to high density of fluorescent spots whose overlap precluded single-molecule tracking.

An alternative explanation for our observation of large areas with low occupancy and short residence times on hydrophobic HDPE films at high Fg concentration is that oriented layers form only in the areas in which we observe elongated occupancy maps, perhaps due to heterogeneity in the underlying HDPE film. This seems unlikely to be the case, however, given the observation that oriented crystalline lamellae cover a large area fraction of the HDPE film, as shown in Figure 2a.

Table 1. Mean residence times on HDPE films.

		Mean Residence Time [s]	
Surface	Fg Concentration [mg L^{-1}]	High Occupancy	Low Occupancy
Pl-HDPE	10	0.9 ± 0.2	0.80 ± 0.02
HDPE	5×10^{-4}	1.4 ± 0.5	1.1 ± 0.1
HDPE	10	>160	1.4 ± 0.2

2.3. Anisotropic Diffusion

We also explored the diffusion of Fg on these HDPE films, analyzing diffusion separately in the directions parallel and perpendicular to the drawing direction (**Figure 4**). As described in the methods section, the diffusion polarization (*P*), which ranges from –1 to 1, is defined such that high positive polarization indicates much faster diffusion in the drawing direction. Again, the MAPT technique allows trajectories from high and low occupancy areas to be analyzed separately. Areas of high occupancy have greater *P* than areas of low occupancy but this trend is most pronounced on hydrophobic HDPE at high Fg concentration. Low absolute values of the polarization indicate nearly isotropic diffusion on hydrophilic HDPE and hydrophobic HDPE films at low Fg concentration. Thus it seems that

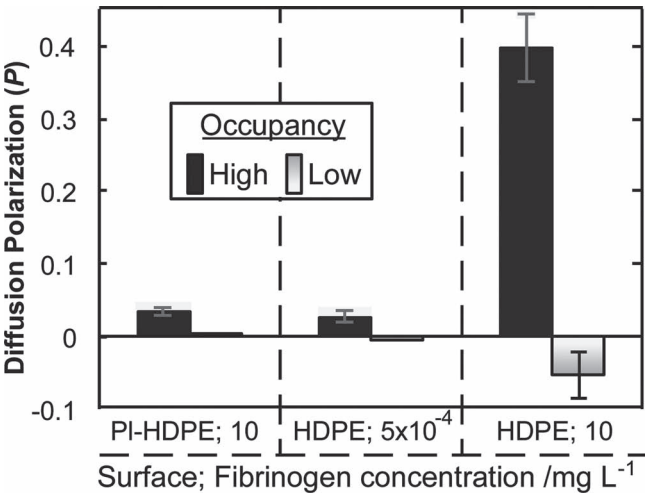

Figure 4. Diffusion polarization on HDPE films. The film treatment and Fg solution, in mg L^{-1} are shown along the bottom. Areas of high occupancy, as seen in Figure 1 and 2 are analyzed separately from areas of low occupancy. Polarization is anomalously high on hydrophobic HDPE exposed to Fg at 10 mg L^{-1}, indicating faster diffusion in the drawing direction.

nanostructured HDPE alone has a minor effect on the direction of Fg diffusion; the ordered layer formation is the major determinant of diffusive motion.

It is also useful to examine the magnitude of the direction-independent diffusion coefficient for the various areas on each HDPE film (**Figure 5**). Diffusion is fastest on hydrophilic HDPE, slower on HDPE at low Fg concentration, and much slower on HDPE at high Fg concentration. In all cases, diffusion slows moderately when moving from areas of low to high occupancy. In the paradigm of a partial detachment model for

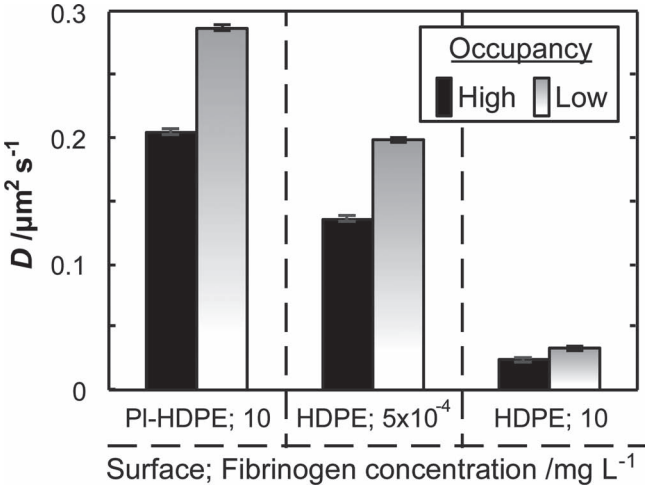

Figure 5. Diffusion coefficient on HDPE films. The film treatment and Fg solution, in mg L^{-1} are shown along the bottom. Areas of high occupancy, as seen in Figure 1 and 2 are analyzed separately from areas of low occupancy. Under all conditions, the diffusion coefficient is lower in areas of high occupancy. Diffusion is much slower on hydrophobic HDPE exposed to Fg at 10 mg L^{-1}.

desorption, where a molecule must break at least some of its surface contacts in order to move at a solid-liquid interface, these trends are qualitatively consistent with those observed for the mean residence time whereby films and regions with slower diffusion have more stable surface contacts and are less likely to desorb.[30,34,35] It is unknown how to quantitatively relate mean residence time to diffusion and thus we cannot further compare observed trends in the two types of dynamic behavior.

Interestingly, although areas of high occupancy on hydrophobic HDPE film have extremely long residence times at high Fg concentration, diffusion, while slow, is nonzero even after correcting for the effects of positional uncertainty (discussed in the Experimental Section). This demonstrates that even in a stable Fg layer whose components do not desorb, individual proteins still have some mobility in the plane of the film. The mechanisms behind this mobility remain unclear at this point. It is perhaps surprising that relatively slow diffusion is also observed in areas of low occupancy on HDPE films at high bulk Fg concentration given that mean residence times and diffusion polarization on these areas are more comparable to hydrophilic HDPE and HDPE at low Fg concentration. This indicates that even for proteins that do not incorporate into the ordered Fg layer, lateral barriers to diffusion are significant and that Fg does not detach completely from the surface when diffusing. Thus, Fg that adsorbs to the film but does not incorporate is able to desorb relatively easily but its lateral motion still feels the effects of the protein layer.

This idea of partial, but not complete, detachment as a mechanism for diffusion in protein films also explains the high value for diffusion polarization in high occupancy areas on HDPE at high Fg concentration. If molecules cannot completely detach from the surface, they cannot "fly" between parallel rows of lamellae, typically separated by a few tens of nanometers without experiencing the (presumably) less favorable interactions with amorphous HDPE. They are effectively confined in one direction, leading to slower apparent diffusion in that direction. In contrast, complete detachment and flights between parallel rows of lamellae might be more prevalent on hydrophilic HDPE and hydrophobic HDPE at low Fg concentration due to the lack of an ordered Fg layer. Diffusion via a flying mechanism would most likely lead to the observed elevated diffusion coefficients and would reduce the barriers to perpendicular diffusion, allowing relatively isotropic diffusion. This analysis again points to the dramatic stabilizing effect of an ordered Fg layer.

3. Conclusions

This work demonstrated the characterization of a nanostructured surface using a probe species of functional interest. Spatially heterogeneous dynamic behavior of accumulated probe trajectories was used to identify differences in surface properties. In particular, we were able to identify specific Fg molecules that had become incorporated into an ordered protein layer within regions of crystalline lamellae by their characteristic long residence times and polarized diffusion. These direct insights into Fg dynamics were a result of single-molecule resolution at low surface coverage of probe Fg, which allowed tracking of

individual proteins with sub-diffraction spatial resolution. In addition, these insights required the ability to group trajectories spatially and by their functional properties as not all observable probe molecules reported on film-incorporated dynamics. Going forward, this work has demonstrated MAPT as a powerful technique for the in situ study of protein layer formation and it may be used to characterize similar processes on a variety of nanostructured materials that are exposed to complex physiological environments. In particular, the ability to fluorescently label individual species in a heterogeneous fluid such as blood plasma may permit a mechanistic dissection of the role of each species in addition to the role of the interface.

Dynamic Fg behavior was relatively similar on hydrophilic HDPE films and HDPE films at low bulk Fg concentration, conditions that had previously been shown to result in disordered network formation. In contrast, the mean residence time of Fg that had incorporated into ordered layers on HDPE films at high bulk protein concentration increased by several orders of magnitude, from ~1 s to several minutes. This important result indicates that nanostructured HDPE and UHMWPE films can have significant benefits for implanted biomaterials by dramatically increasing the residence time of Fg in an ordered protein layer and potentially reducing the wear on the underlying material. Diffusion under these conditions was found to be anisotropic, with Fg moving significantly faster in the drawing direction of the HDPE film. We hypothesize that this was an effect of ordered layer formation, in which large diffusive steps via complete surface detachment and reattachment are essentially eliminated, thus confining individual proteins to a single row of crystalline lamellae. Nevertheless, diffusion in ordered layers was found to be non-zero, indicating some lateral mobility in an otherwise stable protein layer. In future work, anisotropic diffusion may be one property that can indicate ordered protein layer formation.

4. Experimental Section

Fibrinogen Solutions: Unlabeled human plasma fibrinogen was purchased from Calbiochem while human plasma fibrinogen, labeled with AlexaFluor 488, was purchased from Molecular Probes, Inc. Phosphate buffered saline (PBS) was purchased from Invitrogen. Concentrated stocks of these proteins were prepared in PBS, divided into aliquots, and frozen until use. Each aliquot was only thawed once for use in one experiment. Immediately prior to experimental use, Fg/PBS solutions were prepared from thawed stock at a final concentration of labeled Fg of 5×10^{-4} mg L^{-1} (1.5×10^{-12} M) in order to achieve low surface densities for single-molecule experiments. Optionally, unlabeled Fg was added at a concentration of 10 mg L^{-1} (2.9×10^{-8} M). For labeled Fg, the manufacturer-specified degree of labeling was approximately 15 dye molecules per protein, making it unlikely that blinking effects would cause a given protein to disappear during image capture.

Film Preparation and Characterization: As previously described,[11,24] melt-drawn HDPE films were prepared as follows. HDPE pellets (Sigma-Aldrich) were dissolved in xylene (synthesis grade, Merck KGaA) to obtain a 1 wt% polymer solution, which was heated to 120 °C. Subsequently, a few droplets were placed onto a heated glass plate on top of a precision heating plate kept at a temperature of 125 °C. After evaporation of the solvent, an ultrathin, highly oriented polymer film (thickness <100 nm) was drawn from the resulting polymer melt reservoir by a motor-driven cylinder to control the drawing rate at approximately 10 cm s^{-1}. Subsequently, the free-standing polymer film consisting of highly oriented crystalline PE lamellae embedded in the surrounding amorphous matrix was carefully fixed onto a thin fused silica wafer (Mark Optics) to permit fluorescence microscopy. The surface of the HDPE melt-drawn film was characterized by tapping mode AFM at a scan rate of 2 Hz with a Dimension 3100 instrument (Digital Instruments, Santa Barbara, CA) and a Nanoscope IV controller at ambient temperature in air and standard silicon cantilevers (Olympus OMCL-AC160TS, Atomic Force F&E GmbH, Mannheim, Germany) with typical resonance frequency of 300 kHz and a cantilever stiffness of 42 N m^{-1}. Half of the melt-drawn HDPE films were treated by Ar plasma to make them hydrophilic. Ar plasma was applied at a pressure of 0.25 mbar for 60 s by a PDC-32G instrument (Harrick Plasma, New York, USA, radio frequency of 8–12 MHz, power of 10.5 W). Static contact angles of the hydrophilic and hydrophobic HDPE films were 39.9° ± 2.2° and 98.2° ± 1.6°, respectively.

Total Internal Reflection Fluorescence Microscopy: Total internal reflection fluorescence microscopy (TIRFM) measurements were performed using a custom-built prism-based illumination system, flow cell, Nikon TE-2000 microscope with a 60× objective and 491 nm diode-pumped solid state laser that have been described previously.[36] The flow cell was maintained at 37.0 ± 0.1 °C and flow was stopped after introduction of the Fg solution. A 0.2 s frame acquisition time was used and ten 800-frame movies were taken, accumulating over 3×10^5 trajectories on each surface. In TIRFM, the evanescent wave created by total internal reflection has a penetration depth of less than 100 nm and consequently only objects near the surface are excited. While in principle one could resolve individual molecules diffusing in solution, in practice these molecules have diffusion coefficients that are 10^3–10^4 times higher than those at the interface, so the signal due to an individual molecule in solution is negligible in any given pixel. These experimental conditions gave signal-to-noise ratios of 3.5 ± 1 as determined by the maximum intensity of each identified object divided by the root mean squared value of background intensity.

Diffraction-limited objects were identified in each frame via convolution with a disk matrix and thresholding. Objects in each frame were given a specific position in the two-dimensional plane as calculated by their centroid of intensity. That is, the (x,y) position is given by $\left(\sum_i x_i F_i, \sum_i y_i F_i\right)$ where (x_i,y_i) is the position of the i^{th} pixel with intensity, F_i, and i the sum is over all the pixels identified as a single object. Object tracking was then accomplished by identifying the closest objects in sequential frames while requiring the distance between closest objects to be less than 4 pixels (910 nm). Surface residence times were calculated as the number of frames on which the object was identified, multiplied by the exposure time of each frame.

Image Processing and Data Analysis: In order to create surface occupancy maps, the observation area was divided into square bins of user-specified width. The number of frames in which an object was present in this area was counted. Consequently, high occupancy could be the result of one object residing in the same area for many frames or many different objects passing through that area. The occupancy number was then divided by the area of the bin, total observation time, and bulk concentration of labeled Fg as these quantities are expected to be linearly proportional to the observed number of molecules in a given area. As a point of reference, one molecule residing in a bin for 0.2 s (i.e., one frame out of ten 800-frame movies) corresponds to a surface occupancy of 1.3×10^{12} μm^{-2} s^{-1} M^{-1}.

For analysis of residence times, an entire trajectory was sorted by its mean position based on user-defined areas of high and low occupancy. For a given collection of trajectories, the mean surface residence time was simply the sum of all observed residence times divided by the number of observations in that group. The error for this measurement was taken as the standard deviation of the mean value obtained from randomly selecting different subgroups of trajectories from within the larger collection. This estimate of the standard deviation is more meaningful than simply taking the standard deviation of the residence time distribution because the standard deviation of a residence time distribution for a first order process is expected to equal the mean residence time.

For analysis of diffusive motion, each step in a trajectory was placed at the mean location between its starting and ending points. These individual steps were then grouped by position based on user-defined areas of high and low occupancy. Each diffusive step was then separated into its components parallel and perpendicular to the drawing direction of the HDPE film, and the squared-displacement in this direction calculated. The diffusion coefficient in each direction was then estimated as the mean squared-displacement divided by $2\Delta t$ where Δt is the acquisition time of 0.2 s and the factor of 2 is used for diffusion in one dimension. This value is equivalent to the mean diffusion coefficient for a Gaussian random walk with an arbitrary number of distinct diffusive modes. As was done with mean residence times, the error for each measurement of the diffusion coefficient was determined by randomly selecting different subgroups of diffusive steps from within the larger collection of steps. A value of 0.0125 $\mu m^2\ s^{-1}$ was subtracted from the mean diffusion coefficient in both the parallel and perpendicular directions to account for the effects of positional uncertainty. We estimated the positional uncertainty at $\sigma = 50\ nm \pm 1\ nm$ and this adds a value of $\sigma^2/\Delta t$ to the mean diffusion coefficient.[37] Positional uncertainty was estimated by selecting a subset of objects that appeared to be immobilized over long time intervals and observing how fast they appeared to diffuse at $\Delta t = 0.2$ s. Specifically, these immobile molecules did not exhibit a displacement greater than 1 pixel (0.227 μm) at any point during their surface residence time, which was required to be at least 5 s.

After calculating parallel ($D_{\parallel}$) and perpendicular ($D_{\perp}$) diffusion coefficients, these parameters were reduced into the diffusion polarization (P) using Equation 1:

$$P = \frac{D_{\parallel} - D_{\perp}}{D_{\parallel} + D_{\perp}} \quad (1)$$

Additionally, the 2D diffusion coefficient (D) is simply the average of its 1D components as shown in Equation 2:

$$D = \frac{D_{\parallel} + D_{\perp}}{2} \quad (2)$$

Acknowledgements

M.K. and D.K.S. gratefully acknowledge partial support by the National Science Foundation (NSF) award # CHE-0841116, NSF Industry/University Cooperative Research Center for Membrane Science, Engineering and Technology (NSF Award # IIP1034720), the US Department of Energy (DE- SC0001854), and the National Institute of General Medical Sciences (award # 1F32GM091777-02). T.F.K. and K.D.J. gratefully acknowledge the partial support from the BMBF within the project "Innovations- und Gründerlabor für neue Werkstoffe und Verfahren (IGWV)" an der Friedrich-Schiller-Universität Jena, Förderkennzeichen: 03GL0026.

Received: November 23, 2011
Revised: February 22, 2012
Published online: March 29, 2012

[1] N. M. Coelho, C. Gonzalez-Garcia, M. Salmeron-Sanchez, G. Altankov, *Tissue Eng. A* **2011**, *17*, 2245.
[2] M. P. Heuberger, M. R. Widmer, E. Zobeley, R. Glockshuber, N. D. Spencer, *Biomaterials* **2005**, *26*, 1165.
[3] P. Parhi, A. Golas, N. Barnthip, H. Noh, E. A. Vogler, *Biomaterials* **2009**, *30*, 6814.
[4] L. C. Xu, C. A. Siedlecki, *Langmuir* **2009**, *25*, 3675.
[5] K. S. K. Karuppiah, A. L. Bruck, S. Sundararajan, J. Wang, Z. Q. Lin, Z. H. Xu, X. D. Li, *Acta Biomater.* **2008**, *4*, 1401.
[6] A. L. Bruck, K. S. K. Karuppiah, S. Sundararajan, J. Wang, Z. Q. Lin, *J. Biomed. Mater. Res. B* **2010**, *93B*, 351.
[7] A. Dolatshahi-Pirouz, T. Jensen, D. C. Kraft, M. Foss, P. Kingshott, J. L. Hansen, A. N. Larsen, J. Chevallier, F. Besenbacher, *ACS Nano* **2010**, *4*, 2874.
[8] M. S. Lord, M. Foss, F. Besenbacher, *Nano Today* **2010**, *5*, 66.
[9] G. M. L. Messina, C. Satriano, G. Marletta, *Chem. Commun.* **2008**, 5031.
[10] P. E. Scopelliti, A. Borgonovo, M. Indrieri, L. Giorgetti, G. Bongiorno, R. Carbone, A. Podesta, P. Milani, *PLoS One* **2010**, *5*, e11862.
[11] T. F. Keller, M. Muller, W. Y. Ouyang, J. T. Zhang, K. D. Jandt, *Langmuir* **2010**, *26*, 18893.
[12] R. Walder, N. Nelson, D. K. Schwartz, *Nat. Commun.* **2011**, *2*, 515.
[13] R. Walder, N. Nelson, D. K. Schwartz, *Phys. Rev. Lett.* **2011**, *107*, 156102.
[14] H. Cang, A. Labno, C. G. Lu, X. B. Yin, M. Liu, C. Gladden, Y. M. Liu, X. Zhang, *Nature* **2011**, *469*, 385.
[15] R. Jungmann, C. Steinhauer, M. Scheible, A. Kuzyk, P. Tinnefeld, F. C. Simmel, *Nano Lett.* **2010**, *10*, 4756.
[16] A. Sharonov, R. M. Hochstrasser, *Proc. Natl. Acad. Sci. USA* **2006**, *103*, 18911.
[17] D. M. Wu, Z. W. Liu, C. Sun, X. Zhang, *Nano Lett.* **2008**, *8*, 1159.
[18] R. Walder, D. K. Schwartz, *Soft Matter* **2011**, *7*, 7616.
[19] K. Nishimura, R. Mori, W. Miyamoto, Y. Uchio, *Clin. Biomech.* **2009**, *24*, 403.
[20] R. A. Schindler, H. B. Gladstone, N. Scott, G. T. Hradek, H. Williams, S. B. Shah, *Am. J. Otol.* **1995**, *16*, 304.
[21] E. Wintermantel, S.-W. Ha, *Medizintechnik: Life Science Engineering*. Springer, Berlin **2009**.
[22] Y. Zhang, K. E. Tanner, *J. Mater. Sci.: Mater. Med.* **2008**, *19*, 761.
[23] T. Keller, M. Grosch, K. D. Jandt, *Macromolecules* **2007**, *40*, 5812.
[24] T. F. Keller, J. Schonfelder, J. Reichert, N. Tuccitto, A. Licciardello, G. M. L. Messina, G. Marletta, K. D. Jandt, *ACS Nano* **2011**, *5*, 3120.
[25] D. S. Gibson, M. E. Rooney, *Proteomics: Clin. Appl.* **2007**, *1*, 889.
[26] N. Chang, A. Bellare, R. E. Cohen, M. Spector, *Wear* **2000**, *241*, 109.
[27] M. Ohta, S. H. Hyon, Y. B. Kang, M. Oka, S. Tsutsumi, S. Murakami, S. Kohjiya, *JSME Int. J. Ser. C* **2003**, *46*, 1297.
[28] D. C. Wirtz, E. Schopphoff, D. Weichert, F. U. Niethard, *Biomed. Tech.* **2001**, *46*, 338.
[29] K. S. K. Karuppiah, S. Sundararajan, Z. H. Xu, X. D. Li, *Tribol. Lett.* **2006**, *22*, 181.
[30] M. Kastantin, B. B. Langdon, D. L. Chang, D. K. Schwartz, *J. Am. Chem. Soc.* **2011**, *133*, 4975.
[31] M. W. Mosesson, K. R. Siebenlist, J. P. Diorio, M. Matsuda, J. F. Hainfeld, J. S. Wall, *J. Clin. Invest.* **1995**, *96*, 1053.
[32] G. J. Chen, N. T. Ni, B. H. Wang, B. Q. Xu, *ChemPhysChem* **2010**, *11*, 565.
[33] P. S. Sit, R. E. Marchant, *Thromb. Haemostasis* **1999**, *82*, 1053.
[34] M. Kastantin, D. K. Schwartz, *ACS Nano* **2011**, *5*, 9861.
[35] A. Honciuc, D. K. Schwartz, *J. Am. Chem. Soc.* **2009**, *131*, 5973.
[36] A. Honciuc, A. W. Harant, D. K. Schwartz, *Langmuir* **2008**, *24*, 6562.
[37] M. Kastantin, D. K. Schwartz, unpublished.